Monthly Notices
of the
ROYAL ASTRONOMICAL SOCIETY

Mon. Not. R. Astron. Soc. **411,** 1167–1176 (2011) doi:10.1111/j.1365-2966.2010.17749.x

Atmospheric parameters and pulsational properties for a sample of δ Sct, γ Dor and hybrid *Kepler* targets⋆

G. Catanzaro,[1]† V. Ripepi,[2] S. Bernabei,[3] M. Marconi,[2] L. Balona,[4] D. W. Kurtz,[5] B. Smalley,[6] W. J. Borucki,[7] H. Bruntt,[8,9] J. Christensen-Dalsgaard,[9] A. Grigahcène,[10] H. Kjeldsen,[9] D. G. Koch,[7] M. J. P. F. G. Monteiro,[10] J. C. Suárez,[11] R. Szabó[12] and K. Uytterhoeven[13]

[1]*INAF-Osservatorio Astrofisico di Catania, Via S.Sofia 78, I-95123 Catania, Italy*
[2]*INAF-Osservatorio Astronomico di Capodimonte, Via Moiariello 16, I-80131 Napoli, Italy*
[3]*INAF-Osservatorio Astronomico di Bologna, Via Ranzani 1, I-40127 Bologna, Italy*
[4]*South African Astronomical Observatory, PO Box 9, Observatory 7935, Cape Town, South Africa*
[5]*Jeremiah Horrocks Institute of Astrophysics, University of Central Lancashire, Preston PR1 2HE*
[6]*Astrophysics Group, Keele University, Keele, Staffordshire ST5 5BG*
[7]*NASA Ames Research Center, MS 244-30, Moffett Field, CA 94035, USA*
[8]*Observatoire de Paris, LESIA, 5 place Jules Janssen, 92195 Meudon Cedex, France*
[9]*Department of Physics and Astronomy, Building 1520, Aarhus University, 8000 Aarhus C, Denmark*
[10]*Centro de Astrofísica and Faculdade de Ciências, Universidade do Porto, Rua das Estrelas, 410-762 Porto, Portugal*
[11]*Instituto de Astrofísica de Andalucía (CSIC). Rotonda de la Astronomía S/N. Granada, Spain*
[12]*Konkoly Observatory of the Hungarian Academy of Sciences, PO Box 67, 1525 Budapest, Hungary*
[13]*Laboratoire AIM, CEA/DSM-CNRS-Université Paris Diderot; CEA, IRFU, SAp, centre de Saclay, 91191 Gif-sur-Yvette, France*

Accepted 2010 September 21. Received 2010 September 21; in original form 2010 June 4

ABSTRACT

We report spectroscopic observations for 19 δ Sct candidates observed by the *Kepler* satellite both in long and short cadence mode. For all these stars, by using spectral synthesis, we derive the effective temperature, the surface gravity and the projected rotational velocity. An equivalent spectral-type classification has been also performed for all stars in the sample. These determinations are fundamental for modelling the frequency spectra that will be extracted from the *Kepler* data for asteroseismic inference. For all the 19 stars, we also present periodograms obtained from *Kepler* data. We find that all stars show peaks in both low- (γ Dor; g-mode) and high-frequency (δ Sct; p-mode) regions. Using the amplitudes and considering 5 cycles d^{-1} as a boundary frequency, we classified three stars as pure γ Dor, four as γ Dor–δ hybrid Sct, five as δ Sct–γ Dor hybrid and six as pure δ Sct. The only exception is the star KIC 05296877, which we suggest could be a binary.

Key words: stars: early-type – stars: fundamental parameters – stars: oscillations.

1 INTRODUCTION

Stellar pulsations offer a unique opportunity to constrain the intrinsic parameters of stars and, by using asteroseismology, to unveil their inner structure. In particular, the classical δ Sct variables are late A-type and early F-type stars that populate the instability strip between the zero-age main sequence (ZAMS) and terminal-age main sequence, with $3.0 \leq M_V \leq 0.5$. They pulsate in mode of low radial order with periods ranging from about 20 min to 8 h (see Breger 2000, for a review). δ Sct stars pulsate in both radial and non-radial p modes and g modes, driven by the κ-mechanism, in particular in the He II ionization zone. The γ Dor variables, with periods between about 0.3 and 3 d, are mostly located near the cool edge of the δ Sct instability strip (Kaye et al. 1999). Their pulsations are driven by convective blocking at the base of their envelope convection zone (Guzik et al. 2000; Dupret et al. 2004; Grigahcène et al. 2004). The distinction between the two classes is clearer, if we consider the value of the pulsation constant Q (Handler & Shobbrook 2002). However, the location of the γ Dor stars in the Hertzsprung–Russell (HR) diagram suggests some relationship with the δ Sct variables. Indeed, stars exist, which show simultaneously both δ Sct and γ Dor pulsations (Henry & Fekel 2005; King et al. 2006; Rowe et al. 2006; Uytterhoeven et al. 2008a; Handler 2009). These hybrid objects are in principle of great interest, because they offer additional constraints on stellar structure.

⋆This work is based on spectra taken at the Loiano (INAF - OA Bologna) and Serra La Nave (INAF - OA Catania) Observatories.
†E-mail: gca@oact.inaf.it

Table 1. List of studied *Kepler* δ Sct candidates. Columns (1) and (2) show the *Kepler* and other identifications, respectively; column (3) reports the origin of the spectrum: L = Loiano, OACT = INAF - OACT; and columns (4), (5) and (6) report the V magnitudes, the colour excess and the spectral types taken from the literature.

KIC ID	Other ID	Observatory	V (mag)	$E(B-V)$ (mag)	Spectral type
(1)	(2)	(3)	(4)	(5)	(6)
03219256	HD 178306	L, OACT	8.31	0.02 ± 0.01^a	A3[f]
03429637	HD 178875	OACT	7.72	0.04 ± 0.02^b	A9, Am[g]
03437940	HD 181569	L, OACT	8.45	0.06 ± 0.01^a	F0[f]
04570326	HAT 199−01905	L	9.77	0.00 ± 0.02^c	A2[h]
05296877	HAT 199−27597	L	12.50	0.00 ± 0.02^c	
05724440	HD 187234	L, OACT	7.90	0.06 ± 0.01^a	A5[h]
05965837	HAT 199−00623	L	9.23	0.01 ± 0.02^c	F2[f]
05988140	HD 188774	L	8.83	0.07 ± 0.01^a	F0[f]
07119530	HD 183787	L	8.45	0.02 ± 0.01^a	A3[f]
07798339	HD 173109	L, OACT	7.87	0.00 ± 0.01^a	F0[i]
08197788	NGC 6866-V1	L	12.98	0.12 ± 0.02^d	
08264404	NGC 6866-V3	L	12.22	0.12 ± 0.02^d	
08264698	NGC 6866-V2	L	12.38	0.12 ± 0.02^d	
08583770	HD 189177	L	10.16	0.17 ± 0.03^c	B9[j]
09655114	NGC 6811-RH35	L	12.09	0.12 ± 0.02^e	A4[k]
09775454	HD 185115	L, OACT	8.19	0.01 ± 0.01^a	F1IV[l]
11402951	HD 183489	L, OACT	8.14	0.03 ± 0.01^b	A9, Am[g]
11445913	HD 178327	L, OACT	8.46	0.03 ± 0.01^b	A9, Am[g]
11973705	HD 234999	L	9.10	0.00 ± 0.02^c	B9[f]

[a]From *uvbyβ* photometry. [b]From $(b-y)$ photometry. [c]From $(B-V)$ photometry. [d]Dutra & Bica (2000). [e]Glushkova et al. (1999). [f]SIMBAD. [g]Abt (1984). [h]Fehrenbach & Burnage (1990). [i]Nordstrom et al. (1997). [j]Couteau & Gili (1994). [k]Lindoff (1972). [l]Duflot, Figon & Meyssonnier (1995).

Indeed, the γ Dor stars pulsate in g modes, which have high amplitudes deep in the star and allow us to probe the stellar core, while the p modes, efficient in δ Sct stars, have high amplitudes in the outer regions of the star and probe the stellar envelope. Moreover, since γ Dor stars pulsate in g modes of high radial order, the asymptotic approximation predicts regular patterns in the periods, which, in principle, can be used to determine the spherical harmonic degree. Hybrids thus provide a unique opportunity for asteroseismology, which is not available in pure δ Sct stars (Handler & Shobbrook 2002). Recently, a large separation-like feature has been discovered in the δ Sct star HD 174936 by García Hernández et al. (2009) using *CoRot* data. In that work, such a regularity was used to constrain the modelling of this star. It is extremely interesting to search for such regularities in hybrid stars, for which the presence of other frequency regimes definitely may help the overall comprehension of the pulsational behaviour of these objects.

The *Kepler* satellite[1] was launched on 2009 March 6 and will continuously monitor the brightness of over 100 000 stars for at least 3.5 yr in a 105-deg^2 fixed field of view near the plane of the Milky Way between Deneb and Vega. The main aim of the mission is to detect extrasolar planets, particularly Earth-sized planets in the habitable zone of their stars, where water may be liquid, by the transit method (Borucki et al. 1997). To accomplish this goal, *Kepler* is capable of measuring the stellar brightnesses to μmag precision (Gilliland et al. 2010), which, together with the long duration of the observations, make the data ideal for asteroseismology. Most of the observations are long-cadence (29.4-min) exposures, though a small allocation is available for short-cadence (1-min) exposures. The long-cadence as well as some short-cadence data released to the Kepler Asteroseismic Science Consortium (KASC) have been surveyed for δ Sct and/or γ Dor stars. The long-cadence data are not always suitable for a detailed study of δ Sct oscillations, because many of these stars have frequencies higher than the Nyquist frequency (24.5 cycles d^{-1}) for 29.4-min sampling. These data are, however, suitable for the detection of δ Sct–γ Dor hybrids.

The early KASC data releases led to the discovery of the 19 candidate δ Sct stars listed in Table 1; many more have been found in subsequent data releases, and ground-based studies of these stars are now in progress. Interestingly, many objects show periodograms with frequencies both in the p-mode δ Sct and g-mode γ Dor domains, that is, they are candidate hybrid pulsators (Grigahcène et al. 2010). Dedicated short-cadence *Kepler* data for the most promising hybrid candidates will be exploited for seismic studies of these stars. To this end, it is extremely important to constrain the fundamental parameters of the stars (effective temperature $T_{\rm eff}$, surface gravity $\log g$, projected rotational velocity $v \sin i$, luminosity $\log L/L_\odot$) in order to limit the range of models. Measurement of $v \sin i$ is essential to constrain the rotational velocity of the models. Stellar fundamental parameters can be obtained by using photometry, for example, in the Strömgren system, or by means of mid- or high-resolution spectroscopic observations. Very few of the 19 *Kepler* δ Sct stars have previously been observed spectroscopically and no reliable estimates of the stellar parameters can be derived from the existing data. For this reason, we undertook a systematic spectroscopic study of these *Kepler* targets and report our results here. This work fits in the ground-based observational efforts of the KASC with the aim to characterize all *Kepler* pulsators (Uytterhoeven et al. 2010a,b).

2 OBSERVATIONS AND DATA REDUCTION

The spectra used in our analysis were acquired with two different instruments:

[1] http://kepler.nasa.gov/

Table 2. Comparison of fundamental parameters obtained from spectroscopy and photometry, columns (2)–(6). In column (2), we report the equivalent spectral type, that is, the spectral type assigned to the stars by comparing the spectroscopic $T_{\rm eff}$ with the table in Schmidt-Kaler (1982).

KIC ID	Equivalent spectral type	$v \sin i$ (km s^{-1})	$T_{\rm eff}^{\rm Spec}$ (K)	$T_{\rm eff}^{(V-K)}$ (K)	$T_{\rm eff}^{uvby\beta}$ (K)	$T_{\rm eff}^{\rm IRFM}$ (K)	$T_{\rm eff}^{\rm KIC}$	$\log g^{\rm Spec}$ (cm s^{-2})	$\log g^{uvby\beta}$ (cm s^{-2})	$\log g^{KIC}$ (cm s^{-2})
(1)	(2)	(3)	(4)	(5)	(6)	(7)	(8)	(9)	(10)	(11)
03219256	A8V	90 ± 5	7500 ± 150	7450 ± 150	7650 ± 250	7450 ± 150	7300 ± 250	3.6 ± 0.1	4.1 ± 0.3	3.6 ± 0.3
03429637	F0III	50 ± 5	7100 ± 150	7650 ± 200		7400 ± 150	6950 ± 250	3.0 ± 0.2		3.4 ± 0.3
03437940	A7.5V	120 ± 5	7700 ± 120	7800 ± 150	7850 ± 250	7900 ± 150	7400 ± 250	4.1 ± 0.2	3.7 ± 0.3	3.9 ± 0.3
04570326	F1V	80 ± 20	7000 ± 150	6600 ± 200		6900 ± 150		4.0 ± 0.3		
05296877	F4.5IV	200 ± 20	6500 ± 200	6000 ± 400		6500 ± 150	6650 ± 250	3.8 ± 0.3		4.1 ± 0.3
05724440	A9IV	220 ± 5	7350 ± 120	7700 ± 150	8150 ± 250	7850 ± 150	7300 ± 250	3.6 ± 0.3	4.2 ± 0.3	3.6 ± 0.3
05965837	F1V	20 ± 10	6975 ± 200	6700 ± 200		6850 ± 150	6500 ± 250	4.0 ± 0.4		4.1 ± 0.3
05988140	A9IV	70 ± 20	7400 ± 150	7750 ± 150	7900 ± 250	7900 ± 150	7450 ± 250	3.7 ± 0.3	3.7 ± 0.3	3.5 ± 0.3
07119530	A8IV	200 ± 20	7500 ± 200	7750 ± 150	7800 ± 250	7850 ± 150	7800 ± 250	3.6 ± 0.3	3.3 ± 0.3	3.5 ± 0.3
07798339	F3IV	15 ± 5	6700 ± 200	6900 ± 150	6800 ± 250	6900 ± 150	6700 ± 250	3.7 ± 0.3	3.7 ± 0.3	3.4 ± 0.3
08197788	A8V	230 ± 20	7500 ± 150	7700 ± 200		7950 ± 150	8000 ± 250	4.0 ± 0.3		4.0 ± 0.3
08264404	A8IV	250 ± 20	7500 ± 200	7500 ± 200		7950 ± 150	7900 ± 250	3.7 ± 0.3		3.7 ± 0.3
08264698	A8V	210 ± 20	7500 ± 200	7650 ± 200		8000 ± 150	8000 ± 250	3.9 ± 0.2		3.8 ± 0.3
08583770	A2III	130 ± 10	9000 ± 200	8200 ± 300		8750 ± 200	7650 ± 250	3.0 ± 0.2		3.5 ± 0.3
09655114	A9V	150 ± 20	7400 ± 200	7850 ± 250		7700 ± 150	7750 ± 250	3.9 ± 0.3		3.8 ± 0.3
09775454	F1V	70 ± 5	7050 ± 150	7150 ± 150	7300 ± 250	7050 ± 150		4.0 ± 0.3	4.0 ± 0.3	
11402951	F0IV	100 ± 5	7150 ± 120	7450 ± 150		7450 ± 150		3.5 ± 0.1		
11445913	F0IV	50 ± 5	7200 ± 120	7150 ± 150		7150 ± 150	6950 ± 250	3.5 ± 0.2		3.9 ± 0.3
11973705	A9.5V	120 ± 20	7300 ± 300	7350 ± 200		7400 ± 150	7400 ± 250	4.2 ± 0.3		4.0 ± 0.3

(i) *Loiano Observatory:* we used the Bologna Faint Object Spectrograph & Camera (BFOSC) instrument attached to the 1.5-m Loiano telescope.[2] We adopted the echelle configuration with Grism #9 and #10 (as cross-dispersers). The typical resolution was $R \sim 5000$. Spectra were recorded on a back-illuminated (EEV) CCD with 1300×1300 pixels of 20 μm size, typical readout noise of 1.73 e$^-$ and gain of 2.1 e$^-$/ADU. Observations were carried out during the nights of 2009 September 8–11. The exposure times ranged from 1200 to 3600 s for the brightest and faintest targets, respectively.

(ii) *INAF - OACT:* the 91-cm telescope of the Istituto Nazionale di Astrofisica – Osservatorio Astrofisico di Catania (INAF–OACT) was used to carry out spectroscopy of eight of the targets. The telescope is fibre linked to a REOSC[3] echelle spectrograph, giving $R \sim 20\,000$ spectra in the range 4300–6800 Å. The resolving power was checked using the Th–Ar calibration lamp. Spectra were recorded on a thinned, back-illuminated (SITE) CCD with 1024×1024 pixels of 24 μm size. The typical readout noise was 6.5 e$^-$ at a gain of 2.5 e$^-$/ADU. Observations were carried out during five nights: 2009 September 28, 29, 30 and November 19 and 28. Exposure times were fixed for all the stars at 1 h.

The reduction of spectra, which included the subtraction of the bias frame, trimming, correcting for the flat-field and the scattered light, the extraction of the orders, and the wavelength calibration, was done by using the NOAO/IRAF package.[4] The amount of scattered light correction was about 10 ADU. The signal-to-noise ratio of the spectra was at least ∼130 and 80 for Loiano and OACT observatories, respectively.

[2] http://www.bo.astro.it/loiano/index.htm

[3] REOSC is the Optical Department of the SAGEM Group.

[4] IRAF is distributed by the National Optical Astronomy Observatory, which is operated by the Association of Universities for Research in Astronomy, Inc.

3 PHYSICAL PARAMETERS

3.1 Parameters from photometry: $T_{\rm eff}$ and $\log g$

Complete Strömgren–Crawford $uvby\beta$ photometry is available for seven objects in our sample (stars marked with an ^{a} in column 5 of Table 1), while $uvby$ data are present for three additional objects (stars marked with ^{b} in column 5 of Table 1). The source of both the Strömgren and Strömgren–Crawford data is Hauck & Mermillod (1998). For the other six objects (identified with a ^{c} in column 5 of Table 1) plus the three stars in NGC 6866, only Johnson photometry is available, mainly in BV filters. For these stars, we used the values reported by the SIMBAD. In the near-infrared, JHK photometry of good quality is present in the Two-Micron All-Sky Survey (2MASS) catalogue (Skrutskie et al. 1996) for all the targets.

For the seven stars with $uvby\beta$ photometry, $E(b-y)$ can be estimated by using the calibration by Moon (1985), using the IDL code UVBYBETA. The result is reported in Table 1, where we have used the transformation $E(B-V) = 1.4\,E(b-y)$ (Cardelli, Clayton & Mathis 1989). For the three stars without β indices, we used the equivalent spectral type derived in Section 3.2 to derive the intrinsic $(b-y)$ from the relation between $(b-y)_0$ and spectral type (Voigt 2006). Similarly, for five stars with $(B-V)$ colours, we adopted the intrinsic $(B-V)_0$ colours as a function of spectral type (Schmidt-Kaler 1982). We assigned a larger error to these values than those based on $uvby\beta$ photometry. The remaining four variables are cluster members, three belong to NGC 6866 and one to NGC 6811. The reddenings of these two clusters were adopted from Dutra & Bica (2000) for NGC 6866 and Glushkova, Batyrshinova & Ibragimov (1999) and Luo et al. (2009) for NGC 6811.

Values of $T_{\rm eff}$ and $\log g$ were estimated from c_0 and β using the data grid by Moon & Dworetsky (1985). Typical photometric errors (0.015 and 0.03 mag in β and c_0, respectively) have been assumed. The derived values of $T_{\rm eff}$ and $\log g$ are reported in Table 2 (columns 6 and 10, respectively). In calculating the uncertainties, we conservatively assumed an error of 250 K and 0.3 dex for $T_{\rm eff}$ and $\log g$, respectively. The values of $T_{\rm eff}$ and $\log g$ derived from

spectroscopy (see Section 3.2 below) and *uvbyβ* are in good agreement, with all the differences less than 3σ. Only KIC 05724440 (HD 187234) shows a difference in temperature close to the edge of this limit. We discuss this object in Section 3.3.

An additional photometric estimate of $T_{\rm eff}$ can be obtained from the calibrations by Masana, Joedi & Ribas (2006). These are based on the $(V-K)_0$ colour as well as on $\log g$ and [Fe/H]. The V and K bands were taken from the SIMBAD and 2MASS catalogues, respectively. For $\log g$, we use the value from our spectroscopy. For the metallicity, following Bruntt, De Cat & Aerts (2008), we adopted [Fe/H] $=-0.2\pm0.2$. This arbitrary value has only a small impact on the results, because varying [Fe/H] by 2σ gives an error of only 40 K in $T_{\rm eff}$. To de-redden the observed $(V-K)$ colours, we adopted the reddening reported in Table 1, using the relation $E(V-K)=3.8\,E(b-y)$ (Cardelli et al. 1989) for the stars with Strömgren photometry and $E(V-K)=2.8\,E(B-V)$ for the other stars. The resulting $T_{\rm eff}$ and the relative errors are reported in Table 2 (column 5). In general, there is good agreement between the photometric and spectroscopic values.

Near-infrared photometry from the 2MASS, complemented by the one in the optical, can be used to derive an alternative estimate of $T_{\rm eff}$ by means of the infrared flux method (IRFM, Blackwell & Shallis 1977). In particular, broad-band photometry (this work, plus TASS4 I-mag, NOMAD R-mag, CMC14 r'-mag and 2MASS photometry) was used to estimate the total observed bolometric flux ($f_{\rm tot}$). The photometry was converted to fluxes and the best-fitting Kurucz (1993b) model flux distribution was found and integrated to determine $f_{\rm tot}$. The IRFM (Blackwell & Shallis 1977) was then used with 2MASS fluxes to determine the $T_{\rm eff}$ reported in Table 2 (column 7).

Finally, we inspected the Kepler Input Catalogue (KIC,[5] Latham et al. 2005), where additional estimates for $T_{\rm eff}$ and $\log g$ based mainly on u', g', r', i', z'[6] are present. These values are reported in columns (8) and (11) of Table 2. It is worth noting that the KIC catalogue was mainly aimed at separating dwarfs from giants; therefore, the values of $T_{\rm eff}$ and $\log g$ are not expected to be very precise. Since no errors are present in the KIC catalogue, we assumed uncertainties of 250 K and 0.3 dex in $T_{\rm eff}$ and $\log g$, respectively.

3.2 Parameters from spectroscopy: $T_{\rm eff}$, $\log g$ and rotational velocities

We determined $T_{\rm eff}$ and $\log g$ of the stars by minimizing the difference between the observed and the synthetic Hβ profiles. For the goodness-of-fit parameter, we used χ^2 defined as

$$\chi^2=\frac{1}{N}\sum\left(\frac{I_{\rm obs}-I_{\rm th}}{\delta I_{\rm obs}}\right)^2,$$

where N is the total number of points, $I_{\rm obs}$ and $I_{\rm th}$ are the intensities of the observed and computed profiles, respectively, and $\delta I_{\rm obs}$ is the photon noise. The errors have been estimated from the variation in the parameters required to increase χ^2 by 1. As starting values of $T_{\rm eff}$ and $\log g$, we used $T_{\rm eff}$ and $\log g$ derived from the photometry, as described in the previous section. At the same time, we determined the projected rotational velocity by matching the Mg II λ4481 Å profile with a synthetic profile. The synthetic profiles are computed with SYNTHE (Kurucz & Avrett 1981) on the basis of ATLAS9 (Kurucz 1993a) local thermodynamic equilibrium (LTE) atmosphere models. All models are calculated using the solar opacity distribution function (ODF), solar metallicity and a microturbulence velocity of $\xi=2\,{\rm km\,s^{-1}}$. The atomic parameters for the spectral lines were taken from Kurucz & Bell (1995).

The derived values of $T_{\rm eff}$, $\log g$ and $v\sin i$ are reported in Table 2 (columns 4, 9 and 3, respectively). The table also shows the equivalent spectral types and luminosity classes derived by comparing these values of $T_{\rm eff}$ and $\log g$ with the tables in Schmidt-Kaler (1982). In Fig. 1, we show the spectra in three different wavelength ranges for two stars observed with both telescopes. The following lines are plotted: Mg II λ4481 Å, Mg I λλ5167 Å, 5172 Å and the 5183 Å triplet, and Hβ. The Mg I triplet was also used to check the derived values of $\log g$ for the coolest stars.

3.3 Comparison between astrophysical parameters derived by different methods

For the 15 stars with spectral types available in the literature (see column 6 of Table 1),[7] we can compare these values with those derived in this paper (column 2 of Table 2). For seven stars there is agreement. For the three stars classified as metallic-lined (Am stars) by Abt (1984), our inferred spectral type agrees with that derived by this author from Balmer lines on the basis of 1-Å resolution spectra. For the remaining five stars, the discrepancy is large, with differences of more than three or four spectral subtypes. This is not surprising because the nature of several classifications in the literature is uncertain or based on photometry. For these stars, we adopt the values from our spectroscopic analysis. The only high-resolution study in the literature is by Nordstrom et al. (1997) for the star KIC 07798339 (HD 173109). These authors analysed echelle spectra in the narrow wavelength range 5165.77–5211.25 Å to obtain $T_{\rm eff}=7000$ K, $\log g=3.5$ and $v\sin i=15.4\,{\rm km\,s^{-1}}$ (no errors available). The difference of 300 K in $T_{\rm eff}$ is not significant within the errors, and the $\log g$ and $v\sin i$ values are in good agreement with our results.

It is useful to compare the values of $T_{\rm eff}$ derived spectroscopically with those obtained via photometric methods [IRFM, $(V-K)$ calibration, KIC]. Inspection of Fig. 2, which illustrates such a comparison, shows a general good agreement among all these values. Quantitatively, a weighted mean of such differences gives $T_{\rm eff}^{\rm Spec}-T_{\rm eff}^{\rm IRFM}=-200\pm200$; $T_{\rm eff}^{\rm Spec}-T_{\rm eff}^{(V-K)}=-130\pm200$; $T_{\rm eff}^{\rm Spec}-T_{\rm eff}^{\rm KIC}=-50\pm300$, non-significant to the 1σ level. Similarly, a very good agreement is found between $T_{\rm eff}^{\rm Spec}$ and $T_{\rm eff}$ estimated through *uvbyβ* photometry (see Table 2). However, there are two exceptions to this trend:

KIC 05724440 (HD 187234): this star shows a large difference between the spectroscopic $T_{\rm eff}$ and that estimated from *uvbyβ* photometry (800 ± 300 K). This difference is at a level of $\approx2.9\sigma$ and deserves some comments. Indeed, there is not a clear explanation for such a large difference. The Loiano and INAF - OACT spectra give exactly the same values for $T_{\rm eff}$ and $\log g$, suggesting that there could be a problem with the photometry. The *uvby* values reported for this star by Hauck & Mermillod (1998) are the average of the measurements by Olsen (1983) and Jordi et al. (1996), while the β value, on which the $T_{\rm eff}$ depends, was measured only by the latter authors. The two quoted *uvby* values are slightly discrepant, but

[5] Accessible via http://archive.stsci.edu/kepler/kepler_fov/search.php

[6] Note, however, that only 25 per cent of the KIC stars have z' photometry and less than 0.1 per cent have u' (see http://nsted.ipac.caltech.edu/data/NStED/kic_columns.html).

[7] KIC 05296877 (HAT 199−27597) and the three objects in NGC 6866 have no spectral type known before.

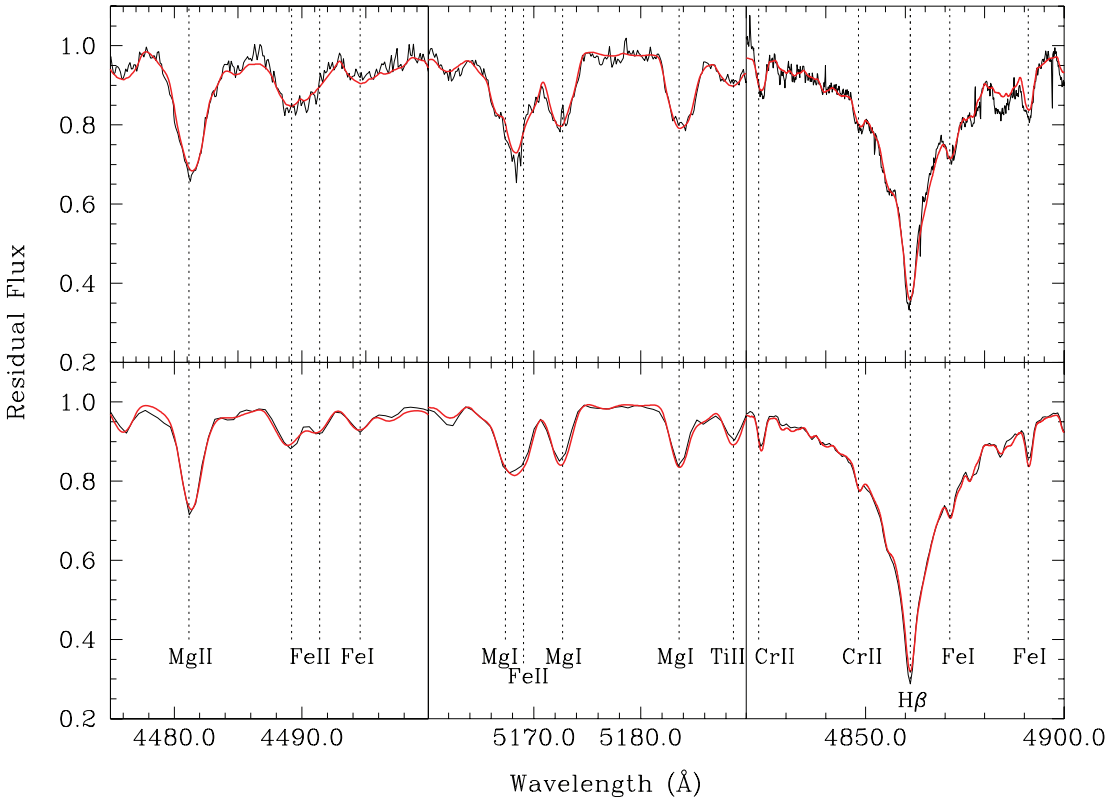

Figure 1. Examples of the fitting procedure for two stars of our sample. The top panel shows three spectral regions of KIC 11402951 (HD 183489) observed with the OACT equipment, while the bottom panel shows the same spectral range, but for KIC 05988140 (HD 188774) observed with the Loiano spectrograph. Both synthetic spectra have been computed with SYNTHE based on LTE ATLAS9 atmospheric models with solar ODF and metallicity.

the difference is not large enough to change significantly the derived value of $\log g$. We also considered the possibility that a close companion is affecting the photometric measurements. We visually inspected both POSS II and 2MASS images of KIC 05724440 (HD 187234), where the star appears to be isolated in the near-infrared. In the optical, it is surrounded by a few very close faint stars whose contribution can hardly be considered significant. By using the calibration by Masana et al. (2006), the discrepancy is reduced to only 350 K, reinforcing our suspicion that there is something wrong with the *uvbyβ* photometry of this star.

KIC 08583770 (HD 189177): $T_{\rm eff} = 9000 \pm 200$ K derived spectroscopically for this star is in good agreement with the value derived from the IRFM and consistent within the errors with $T_{\rm eff}$ derived from $(V - K)$ colour. However, there is a large discrepancy with respect to the KIC estimate. This occurrence could perhaps be explained in terms of a visual binary, with a companion star dimmer by 3 mag at a distance of 0.9 arcsec. Even if nothing is known about the companion, due to the small separation, it is likely that the photometric values are affected by the secondary star flux.

4 THE HR AND $\log g$–$\log T_{\rm eff}$ DIAGRAMS

The stellar parameters $\log g$ and $\log T_{\rm eff}$ determined in the previous section allow us to estimate the luminosity of the investigated objects by interpolating the tables by Schmidt-Kaler (1982). The result is reported in Table 3. Note that the errors on the luminosity were evaluated through the same tables by taking into account the errors on $\log g$ and $\log T_{\rm eff}$. Fig. 3 shows the HR diagram for the 19 stars studied in this work, in comparison with the ZAMS (Pickles 1998), the observed instability strip for δ Sct stars (Breger & Pamyatnykh 1998) as well as the empirical and theoretical red edge of the γ Dor instability strip (Handler & Shobbrook 2002; Warner, Kaye & Guzik 2003). We note that the pulsating variables (see Section 6) are in the expected position, that is, inside the instability strip, except for KIC 08583770 (HD 189177) and KIC 05296877 (HAT 199−27597), which are hotter and cooler than the instability strip, respectively. The former was discussed in the previous section, while the latter is not a pulsating star (see Section 6).

We can use the values of $\log g$ and $\log T_{\rm eff}$ to estimate the mass of the target stars. For this purpose, we used the evolutionary tracks in the BaSTI data base,[8] which are based on the FRANEC evolutionary code (Chieffi & Straniero 1989). We retrieved tracks with both canonical and non-canonical (i.e. with convective overshooting: $\lambda_{\rm OV} = 0.2 H_{\rm p}$) physics in the mass range 1–6 $M_\odot$ with [M/H] = 0.058, $Z = 0.0198$, $Y = 0.273$ and mixing length = 1.913 (Pietrinferni et al. 2004). In Fig. 4, we show the $\log g$– $\log T_{\rm eff}$ diagram. The left-hand and right-hand panels in the figure show canonical and non-canonical tracks, respectively. The resulting masses for the two cases (listed in Table 3) are very similar and agree well within 1σ. On other hand, δ Sct stars are typically fast-rotating objects, and the rotation effects on the structure and evolution might modify the estimates of global parameters of the stars (see e.g. Goupil et al. 2005; Suárez, Bruntt & Buzasi 2005; Fox Machado et al. 2006). To verify if this effect is important in our case, we considered a typical case for a star with mass 1.7–1.8 $M_\odot$. According to Suárez et al. (2005), even in case of

[8] http://albione.oa-teramo.inaf.it/

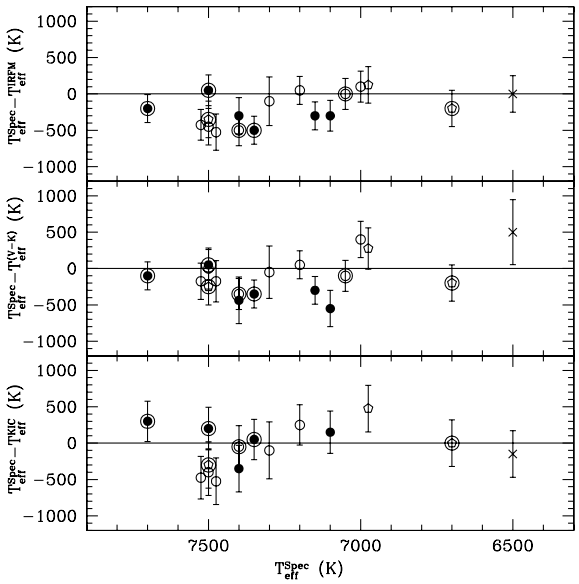

Figure 2. Comparison of $T_{\rm eff}$ obtained spectroscopically and photometrically via the IRFM (top panel), $(V-K)$ (middle panel) and KIC (bottom panel). The filled circles, pentagons and open circles represent variables classified as pure δ Sct, pure γ Dor and hybrids, respectively; the cross shows the candidate W Uma variable (see Section 6 and Table 5). Symbols surrounded by circles refer to stars for which Strömgren photometry is available in the literature (i.e. more precise reddening estimate). Note that for the sake of clarity, the values of $T_{\rm eff}^{\rm Spec}$ of the three stars in NGC 6866 have been shifted by ±25 K. Note also that the star KIC 08583770 (HD 189177) is not visible in the figure, because it lies outside the boundaries of the plots.

$v\sin i \sim 150$–$200\,{\rm km\,s^{-1}}$, the effect on the mass estimate from the HR diagram is of few per cent, well within the uncertainty due to the errors on the empirical estimates of luminosity and effective temperature (see Table 3).

5 CHECKS OF THE RESULTS BY MEANS OF PARALLAXES AND CLUSTER STARS

We used the parallaxes measured by the *Hipparcos* satellite (Perryman et al. 1997) to verify the luminosities derived in this work. We also estimated independently the luminosity of cluster stars by adopting the distances found in the literature obtained through, for example, isochrone fitting.

Only four stars in our sample are sufficiently bright for inclusion in the *Hipparcos* parallax catalogue. These are listed in Table 4 together with the parallaxes from the van Leeuwen (2007) revised catalogue. To derive the luminosity, we used the V and $E(B-V)$ values listed in Table 1 as well as the bolometric correction as a function of spectral type from Pickles (1998). The resulting luminosities and errors are listed in Table 4, where our spectroscopic results are also shown for comparison purposes. An inspection of the table reveals that there is agreement within the errors. The only obvious discrepancy is found for the star KIC 03429637 (HD 178875). The difference in luminosity is $>1\sigma$ and deserves some discussion. We did not find any significant difference between the spectroscopic and the photometric estimates of $T_{\rm eff}$ for this star. Furthermore, the *Hipparcos* parallax (van Leeuwen 2007) is very small relative to the parallax estimated from its spectral type and apparent magnitude. In our opinion, KIC 03429637 (HD 178875) is very likely a double star (Dommanget & Nys 1994). The binary nature can significantly affect the estimated parallax, colour and $T_{\rm eff}$. As mentioned in

Table 3. For each star, the luminosity estimated on the basis of Schmidt-Kaler (1982) tables and the masses estimated from the evolutionary tracks with canonical and non-canonical (i.e. with overshooting) physics, respectively. The errors on the mass and luminosity correspond to the relative precision obtained using the BaSTI data base using non-rotating models. These errors are expected to be different when rotation is considered in the modelling (see text for more details).

KIC	Luminosity $(L/{\rm L}_\odot)$	Mass (canonical) $(M/{\rm M}_\odot)$	Mass (non-canonical) $(M/{\rm M}_\odot)$
03219256	$19.0^{+2.9}_{-2.5}$	$2.20^{+0.20}_{-0.15}$	$2.20^{+0.10}_{-0.10}$
03429637	$20.0^{+6.0}_{-6.0}$	$3.6^{+0.70}_{-0.60}$	$3.2^{+0.60}_{-0.50}$
03437940	$12.5^{+4.0}_{-3.9}$	$1.80^{+0.30}_{-0.20}$	$1.80^{+0.20}_{-0.10}$
04570326	$7.8^{+3.7}_{-3.6}$	$1.70^{+0.20}_{-0.20}$	$1.65^{+0.30}_{-0.15}$
05296877	$7.9^{+2.6}_{-2.6}$	$1.60^{+0.40}_{-0.20}$	$1.70^{+0.25}_{-0.30}$
05724440	$17.0^{+4.4}_{-4.3}$	$2.20^{+0.60}_{-0.40}$	$2.30^{+0.30}_{-0.30}$
05965837	$7.4^{+5.0}_{-4.3}$	$1.70^{+0.30}_{-0.20}$	$1.65^{+0.35}_{-0.15}$
05988140	$16.3^{+4.7}_{-4.6}$	$2.00^{+0.60}_{-0.40}$	$2.20^{+0.30}_{-0.30}$
07119530	$18.8^{+5.4}_{-5.4}$	$2.20^{+0.60}_{-0.40}$	$2.40^{+0.40}_{-0.40}$
07798339	$9.0^{+2.9}_{-2.8}$	$1.80^{+0.30}_{-0.20}$	$1.90^{+0.25}_{-0.30}$
08197788	$12.7^{+4.9}_{-4.8}$	$1.85^{+0.45}_{-0.15}$	$1.80^{+0.40}_{-0.20}$
08264404	$17.4^{+5.5}_{-5.2}$	$2.30^{+0.60}_{-0.45}$	$2.20^{+0.50}_{-0.40}$
08264698	$14.3^{+3.8}_{-3.6}$	$2.00^{+0.30}_{-0.15}$	$1.90^{+0.30}_{-0.20}$
08583770	$65.0^{+19.0}_{-19.0}$	$4.80^{+1.00}_{-0.80}$	$4.40^{+0.80}_{-0.60}$
09655114	$13.5^{+4.7}_{-4.7}$	$1.90^{+0.30}_{-0.30}$	$1.90^{+0.40}_{-0.30}$
09775454	$8.5^{+3.8}_{-3.8}$	$1.70^{+0.20}_{-0.20}$	$1.65^{+0.30}_{-0.15}$
11402951	$15.5^{+2.4}_{-2.7}$	$2.30^{+0.20}_{-0.30}$	$2.20^{+0.10}_{-0.10}$
11445913	$16.3^{+3.2}_{-3.3}$	$1.95^{+0.30}_{-0.10}$	$2.20^{+0.10}_{-0.10}$
11973705	$8.6^{+4.2}_{-4.9}$	$1.60^{+0.30}_{-0.10}$	$1.60^{+0.30}_{-0.15}$

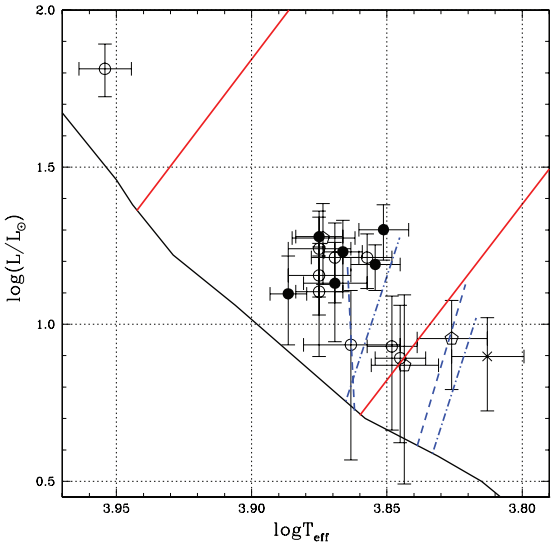

Figure 3. HR diagram for the 19 stars investigated in this paper. Symbols are as in Fig. 2. Note that the values of $T_{\rm eff}$ of KIC 05965837 (HAT 199−00623) were artificially lowered by 25 K to avoid a complete overlap with the star KIC 04570326 (HAT 199−01905). The black solid line is the ZAMS from Pickles (1998); the red solid lines show the δ Sct instability strip by Breger & Pamyatnykh (1998); the blue dashed and dot–dashed lines show the empirical and theoretical red edge of the γ Dor instability strip by Handler & Shobbrook (2002) and Warner et al. (2003), respectively.

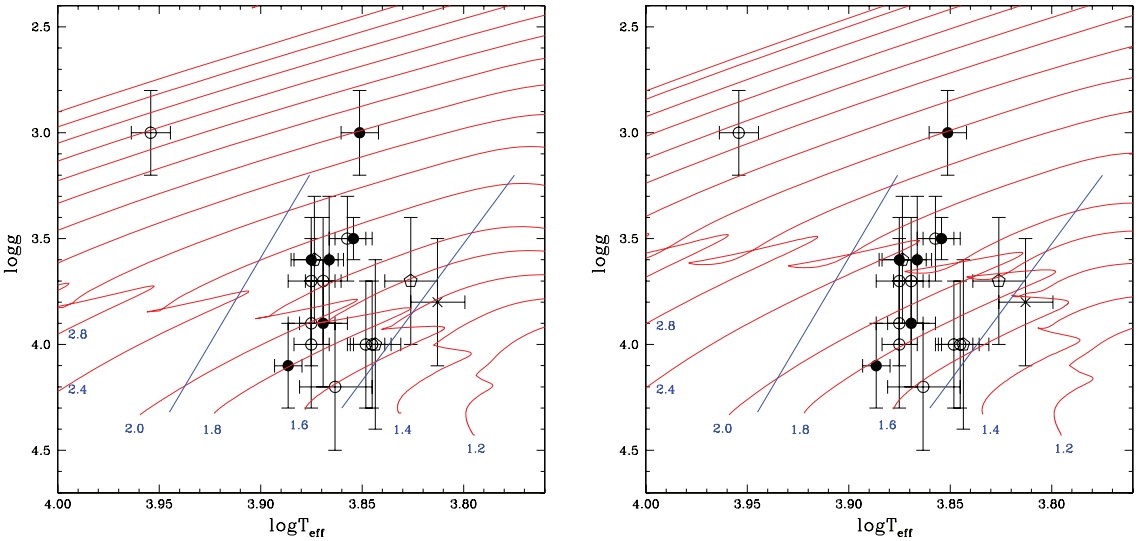

Figure 4. log g– log $T_{\rm eff}$ diagram for the investigated stars. Symbols are as in Fig. 2. For comparison, the instability strip for δ Sct stars by Breger & Pamyatnykh (1998) is shown as straight (blue) lines. The evolutionary tracks for the canonical (left-hand panel) and non-canonical (right-hand panel) physics are also shown. Each track is labelled with the mass (blue number) expressed in $M_\odot$.

Table 4. Comparison between the luminosity derived from present spectroscopy and Schmidt-Kaler (1982) tables and the one obtained from the *Hipparcos* parallaxes or cluster distance (see text).

KIC	π (mas)	$L/L_\odot$ *Hipparcos*	$L/L_\odot$ Spectroscopy
03429637 (HD 178875)	3.75 ± 0.58	$56.2^{+26.3}_{-18.0}$	$20.0^{+6.0}_{-6.0}$
05724440 (HD 187234)	8.02 ± 0.51	$11.1^{+2.1}_{-1.8}$	$17.0^{+4.3}_{-4.3}$
07798339 (HD 173109)	6.86 ± 0.48	$13.4^{+2.8}_{-2.3}$	$9.0^{+2.9}_{-2.8}$
11402951 (HD 183489)	5.91 ± 0.63	$14.9^{+4.4}_{-3.4}$	$15.5^{+2.4}_{-2.7}$
Star	D (pc)	$L/L_\odot$ Cluster	$L/L_\odot$ Spectroscopy
08197788 (NGC 6866-V1)	1200 ± 120	$10.3^{+3.3}_{-2.5}$	$12.7^{+5.0}_{-4.8}$
08264404 (NGC 6866-V3)	1200 ± 120	$20.6^{+6.5}_{-5.0}$	$17.4^{+5.5}_{-5.2}$
08264698 (NGC 6866-V2)	1200 ± 120	$17.9^{+5.7}_{-4.4}$	$14.3^{+3.8}_{-3.6}$
09655114 (NGC 6811-RH35)	1030 ± 50	$17.2^{+5.9}_{-4.4}$	$13.5^{+4.7}_{-4.7}$

Section 3, our spectroscopic determination of $T_{\rm eff}$ is in agreement with that derived by Abt (1984).

As for cluster stars, we have to estimate the distances to the host clusters NGC 6866 and NGC 6811 first.

NGC 6866. As reported by Molenda-Żakowicz (2009), both the distance modulus (DM) and $E(B-V)$ vary significantly from author to author. Here we decided to assume a distance $D = 1200 \pm 120$ pc as in Molenda-Żakowicz (2009) (no error on distance is available in the literature; we assumed conservatively an uncertainty of 10 per cent). As for the reddening, we adopted $E(B-V) = 0.12 \pm 0.02$, according to Dutra & Bica (2000) who made a study of the foreground and background dust in the direction of the cluster. The resulting luminosities for the three variables in NGC 6866 are shown in Table 4 in comparison with our estimates. The agreement is good within the errors.

NGC 6811. Distance modulus and $E(B-V)$ of this cluster were measured by Glushkova et al. (1999) and Luo et al. (2009). They found DM = 10.42 ± 0.03, $E(B-V) = 0.12 \pm 0.02$ and DM = 10.59 ± 0.09, $E(B-V) = 0.12 \pm 0.05$, respectively. To estimate the distance, we made a weighted mean of these results, obtaining $D = 1030 \pm 50$ pc. We then calculated the luminosity for the star KIC 09655114 (NGC 6811–RH35), which is reported in the last row of Table 4. Again, we note the good agreement within the errors with the spectroscopic result.

Table 5. Information on *Kepler* photometry. The first column is the KIC identification. In the second column, the proposed classification is given. The third column gives the number of photometric observations, N. In the fourth column, SC signifies short-cadence (1-min) exposures and LC signifies long-cadence (29.4-min) exposures. The last column gives the length of the data set, Δt, in d.

KIC ID	Type	N	Cadence	Δt (d)
03219256	δ Sct	43 974	SC	30.03
03429637	δ Sct	9870	LC	217.98
03437940	δ Sct	43 989	SC	30.03
04570326	γ Dor–δ Sct	44 010	SC	29.97
05296877	–	14245	SC	9.72
05724440	δ Sct	43 093	SC	30.34
05965837	γ Dor	14 204	SC	9.70
05988140	δ Sct–γ Dor	2099	LC	44.44
07119530	γ Dor	10 340	LC	228.95
07798339	γ Dor	43 254	SC	29.97
08197788	γ Dor–δ Sct	43 370	SC	29.97
08264404	δ Sct–γ Dor	43 375	SC	29.97
08264698	γ Dor–δ Sct	43 348	SC	29.97
08583770	δ Sct–γ Dor	41807	SC	30.79
09655114	δ Sct	38 340	SC	27.11
09775454	δ Sct–γ Dor	10 341	LC	228.95
11402951	δ Sct	14 240	SC	9.72
11445913	δ Sct–γ Dor	14 244	SC	9.72
11973705	γ Dor–δ Sct	14 212	SC	9.72

6 *KEPLER* OBSERVATIONS

Information on *Kepler* observations for the stars studied here is given in Table 5. For 15 out of 19 stars, short-cadence observations are available. From these data, we calculated the periodograms (by using L. Balona's custom software, based on a combination of fast

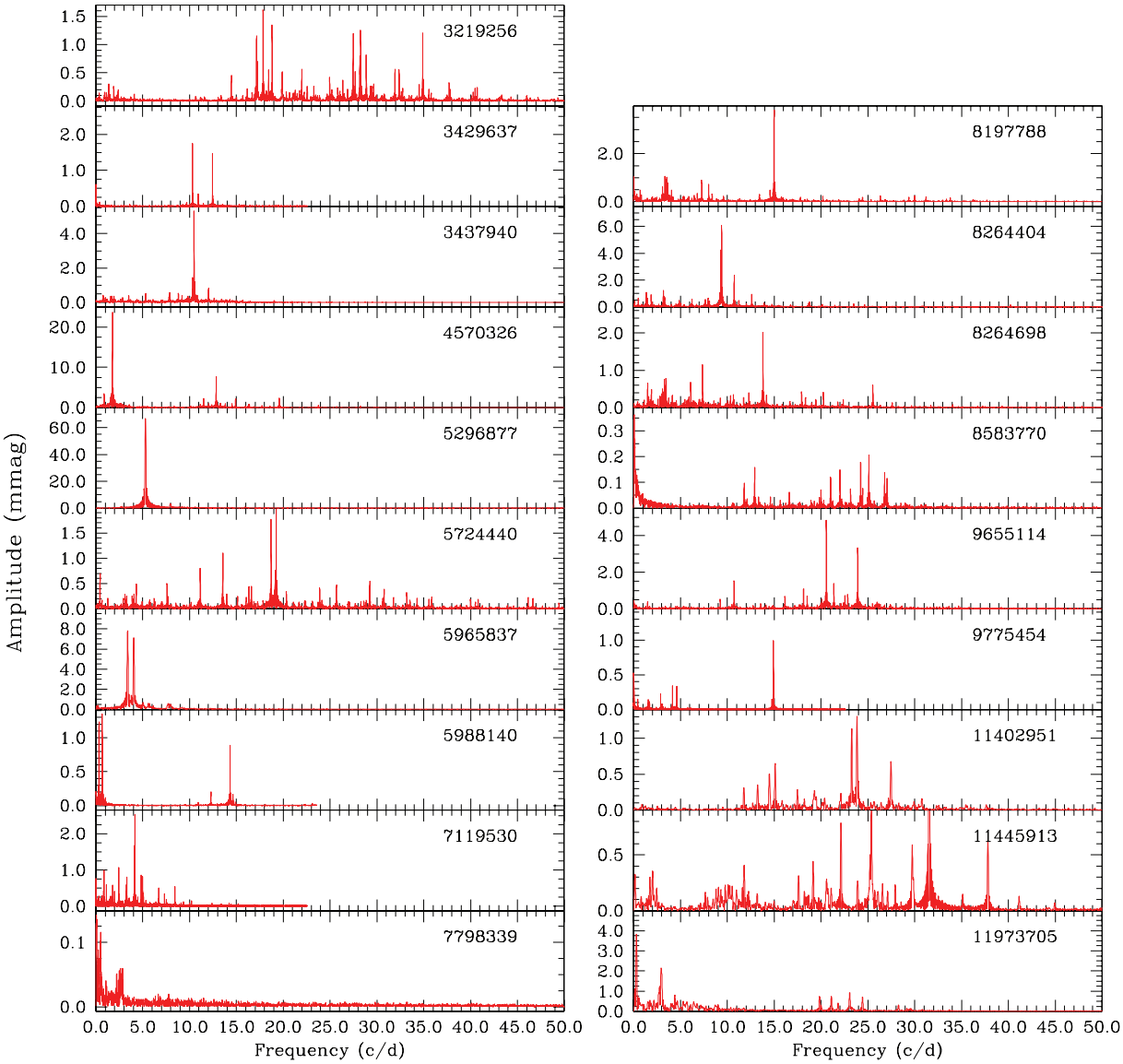

Figure 5. Periodograms of stars of Table 1. The precision in the amplitude of the peaks in these periodograms is typically in the range of 1–10 μmag.

Fourier transform and normal periodogram) shown in Fig. 5. We note that practically all stars show peaks in both the low-frequency (γ Dor; g-mode) and high-frequency (δ Sct; p-mode) regions. In this sense, practically all δ Sct stars observed by *Kepler* are hybrids. This is a surprising finding, which has been discussed in Grigahcène et al. (2010). To make a distinction, we followed the classification scheme proposed by the latter author. We visually classified the stars as δ Sct, if most of the peaks are in the δ Sct region, and as δ Sct–γ Dor, if most of the peaks are in the δ Sct region, but with a significant contribution from the γ Dor region. The frequency 5 cycles d^{-1} was taken as the boundary between the two regions. Following similar arguments, we classify a star as γ Dor or γ Dor–δ Sct. There appears to be a physical significance to such a scheme, as discussed by Grigahcène et al. (2010). We applied these classification criteria to the stars of this study and classified six targets as δ Sct stars, five stars as δ Sct–γ Dor hybrids, four stars as γ Dor–δ Sct hybrids and three stars as pure γ Dor pulsators (see also Table 5). Below we discuss the targets that show particularities in their periodogram (Fig. 5).

KIC 03429637 (HD178875). As noted above, this star shows a $>1\sigma$ difference between the luminosity values derived from the *Hipparcos* parallax and from spectroscopy (see Table 4). Binarity is a possible explanation for this discrepancy. The frequency spectrum shows two dominant peaks near 10 and 12 d^{-1}. A model in terms of δ Sct pulsations, rotation and/or binarity needs to be investigated.

KIC 05296877 (HAT 199−27597). This star is the coolest star in the sample and lies outside the instability strip. The periodogram shows a single strong peak at $f = 5.302$ cycles d^{-1}. KIC 5296877 is probably a contact binary with an orbital period of $2/f = 0.38$ d. The late spectral type of F4.5IV and the large value $v \sin i = 200$ km s^{-1} suggest that it is a high-amplitude ellipsoidal variable.

KIC 07119530 (HD 183787). This star has been classified as pure γ Dor as the frequencies are predominantly in the γ Dor range and those in the δ Sct region have low amplitude. However, the star lies in the middle of the δ Sct instability strip. All the temperature indicators adopted in this paper agree very well with each other and indicate $T_{\rm eff} > 7500$ K, that is, a bit too hot for a pure γ Dor

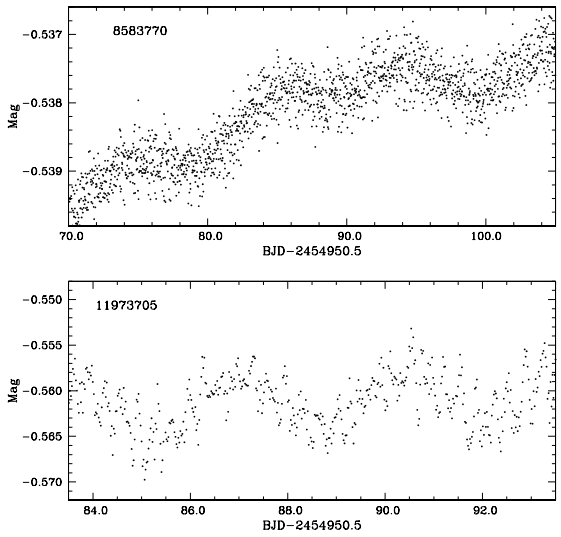

Figure 6. Top panel: light curve of K8583770 (HD 189177). Bottom panel: light curve of K11973705 (HD 234999). The time is expressed in days starting from HJD = 2454950.5 and the brightness is given in mmag.

variable. We conclude that the variability classification of this star is uncertain, since it could be a γ Dor–δ Sct Hybrid.

KIC 08583770 (HD 189177). This star is the hottest star in the group and lies outside the instability strip (see Fig 4). The periodogram shows significant power at very low frequency. The light curve of KIC 08583770 is presented in Fig. 6. No specific period can be deduced, but it is clear that there is something peculiar about this star, which needs further investigation.

KIC 09775454 (HD 185115). The frequency spectrum of KIC 09775454 shows one dominant peak in the δ Sct region, and several – seemingly equidistant – peaks at lower frequencies. Further investigation of the *Kepler* light curves will clarify if this star is a δ Sct star with rotational modulation effects.

KIC 11973705 (HD 234999). The light curves of KIC 11973705 show a periodic long-term behaviour, with $P \approx 4$ d (Fig. 6). The spectral type B9, recorded in the Henry Draper catalogue, is a full spectral class too early to be compared with our classification of A9.5V. It is most likely a δ Sct star in a binary system.

7 SUMMARY

We presented a spectroscopic analysis of 19 candidate δ Sct variables observed by *Kepler* both in long- and short-cadence mode. The analysis is based on medium- to high-resolution spectra obtained at the Loiano and INAF - OACT observatories. For each star, we derived $T_{\rm eff}$, $\log g$ and $v \sin i$ by matching the observed spectra with synthetic spectra computed from the SYNTHE code (Kurucz & Avrett 1981) and using the LTE atmospheric models calculated by ATLAS9 (Kurucz 1993a). The typical errors are about 200 K, 0.2 dex and 10 km s^{-1} for $T_{\rm eff}$, $\log g$ and $v \sin i$, respectively. Equivalent spectral types and luminosity classes were also derived. The luminosities of the stars were obtained using the tables of Schmidt-Kaler (1982).

For 10 stars, we used Strömgren photometry from the literature to estimate the reddening. For seven stars for which β photometry was also available, $T_{\rm eff}$ and $\log g$ could be obtained for comparison with our spectroscopic values. In addition, $V - K$ colours, the IFRM method and values listed in the KIC were used to obtain independent estimates of $T_{\rm eff}$. We find a general good agreement between photometric and spectroscopic results. Four stars with significant parallaxes and four cluster member objects were used to check our estimate of the luminosities. We obtain consistent results for all the stars, with the exception of KIC 03429637 (HD 178875), which is a wide binary and may have an erroneus parallax determination. Moreover, for KIC 05724440 (HD 187234), we suspect a problem with the *uvbyβ* photometry, since $T_{\rm eff}$ derived from the $V - K$ index is in agreement with our estimate within the errors.

Finally, we present the periodograms for the 19 investigated stars, based on the *Kepler* satellite photometry. These beautiful data allowed us to classify the type of variability of each star, including KIC 05296877, which is a high-amplitude ellipsoidal variable candidate. As a result, we find six pure δ Sct, three pure γ Dor and nine hybrid pulsators. This classification is consistent with the derived physical parameters and their position in the HR diagram. As already noted by Grigahcène et al. (2010), we were surprised by the large number of hybrid pulsators. An asteroseismic study of these objects will have a strong impact on our knowledge of the evolution and internal structure of A/F stars. A more in-depth study of the pulsational behaviour of the 18 pulsators is out of the scope of this paper and will be presented in a forthcoming paper.

The stellar parameter estimates for the 18 investigated pulsating stars, presented in this work, will be a fundamental starting point for building proper asteroseismic models aimed at interpreting the frequency spectra extracted from the exceptionally good *Kepler* data.

ACKNOWLEDGMENTS

This work was supported by the Italian ESS project, contract ASI/INAF I/015/07/0, WP 03170 and by the European Helio- and Asteroseismology Network (HELAS), a major international collaboration funded by the European Commission's Sixth Framework Programme.

Funding for the *Kepler* mission is provided by NASA's Science Mission Directorate. We thank the entire *Kepler* team for the development and operations of this outstanding mission.

This research has made use of the SIMBAD data base, operated at CDS, Strasbourg, France. This publication makes use of data products from the 2MASS, which is a joint project of the University of Massachusetts and the Infrared Processing and Analysis Center/California Institute of Technology, funded by the NASA and the National Science Foundation. This work has made use of BaSTI web tools. RS has been supported by the National Office for Reseach and Technology through the Hungarian Space Office Grant No. URK09350 and the LENDÜLET program of the Hungarian Academy of Sciences. MJPFGM and AG are co-supported by project PTDC/CTE-AST/098754/2008 from FCT-Portugal.

REFERENCES

Abt H. A., 1984, ApJ, 285, 247
Blackwell D. E., Shallis M. J., 1977, MNRAS, 180, 177
Borucki W. J., Koch D. G., Dunham E. W. et al., 1997, in Soderblom D. R., ed., ASP Conf. Ser. Vol. 119, Planets Beyond the Solar System and the Next Generation of Space Missions. Astron. Soc. Pac., San Francisco, p. 153
Breger M., 2000, in Breger M., Houston Montgomery M., eds, ASP Conf. Ser. Vol. 210, Delta scuti and Related Stars: Reference Handbook and Proceedings of the 6th Vienna Workshops in Astrophysics. Astron. Soc. Pac., San Francisco, p. 3
Breger M., Pamyatnykh A. A., 1998, A&A, 332, 958
Bruntt H., De Cat P., Aerts C., 2008, A&A, 478, 487
Cardelli J. A., Clayton G. C., Mathis J. S., 1989, ApJ, 345, 245

Chieffi A., Straniero O., 1989, ApJS, 71, 47
Couteau P., Gili R., 1994, A&AS, 106, 377
Dommanget J., Nys O., 1994, Com. de l'Observ. Royal de Belgique, 115, 1
Duflot M., Figon P., Meyssonnier N., 1995, A&AS, 114, 269
Dupret M.-A., Grigahcène A., Garrido R., Gabriel M., Scuflaire R., 2004, A&A, 414, L17
Dutra C. M., Bica E., 2000, A&A, 359, 347
Fehrenbach C., Burnage R., 1990, A&AS, 83, 91
Fox Machado L., Pérez Hernández F., Suárez J. C., Michel E., Lebreton Y., 2006, A&A, 446, 611
García Hernández A., Moya A., Michel E. et al., 2009, A&A, 506, 79
Gilliland R. L., Jenkins J. M., Borucki W. J., 2010, ApJ 712, 160
Glushkova E. V., Batyrshinova V. M., Ibragimov M. A., 1999, Astron. Lett. 25, 86
Goupil M.-J., Dupret M. A., Samadi R., Boehm T., Alecian E., Suarez J. C., Lebreton Y., Catala C., 2005, JA&A, 26, 249
Grigahcène A., Dupret M. A., Garrido R., Gabriel M., Scuflaire R., 2004, Commun. Asteroseismol., 145, 10
Grigahcène A., Antoci V., Balona L. et al., 2010, ApJ, 713, L192
Guzik J. A., Kaye A. B., Bradley P. A., Cox A. N., Neuforge C., 2000, ApJ, 542, L57
Handler G., 2009, MNRAS, 398, 1339
Handler G., Shobbrook R. R., 2002, MNRAS, 333, 2, 251
Hauck B., Mermillod M., 1998, A&AS, 129, 31
Henry G. W., Fekel F. C., 2005, AJ, 129, 2026
Jordi C., Figueras F., Torra J., Asiain R., 1996, A&AS, 115, 401
Kaye A. B., Handler G., Krisciunas K., Poretti E., Zerbi F. M., 1999, PASP, 111, 840
King H., Matthews J. M., Rowe J. F. et al., 2006, Commun. Asteroseismol., 148, 28
Kurucz R. L., Bell B., 1995, Kurucz CD-ROM No. 23. Smithsonian Astrophysical Observatory, Cambridge, MA
Kurucz R. L., 1993a, in Dworetsky M. M., Castelli F., Faraggiana R., eds, IAU Colloq. 138, ASP Conf. Ser. Vol. 44, Peculiar Versus Normal Phenomena in A-Type and Related Stars. Astron. Soc. Pac., San Francisco, p. 87
Kurucz R. L., 1993b, Kurucz CD-ROM 13: ATLAS9. Smithsonian Astrophysical Observatory, Cambridge, MA
Kurucz R. L., Avrett E. H., 1981, SAO Special Rep., 391
Latham D. W., Brown T. M., Monet D. G., Everett M., Esquerdo G. A., Hergenrother C. W., 2005, A&AS 37, 1340
Lindoff U., 1972, A&A, 16, 315
Luo Y. P., Zhang X. B., Luo C. Q., Deng L. C., Luo Z. Q., 2009, New Astron., 14, 584
Masana E., Joedi C., Ribas I., 2006, A&A, 450, 735
Molenda-Żakowicz J., Kopacki G., Steślicki M., Narwid A., 2009, Acta Astron., 59, 193
Moon T. T., 1985, Ap&SS, 117, 261
Moon T. T., Dworetsky M. M., 1985, MNRAS, 217, 305
Nordstrom B., Stefanik R. P., Latham D. W., Andersen J., 1997, A&AS, 126, 21
Olsen E. H., 1983, A&AS, 54, 550
Perryman M. A. C., Lindegren L., Kovalevsky J. et al., 1997, A&A 323, L49
Pickles A. J., 1998, PASP, 110, 863
Pietrinferni A., Cassisi S., Salaris M., Castelli F., 2004, ApJ, 612 168
Rowe J. F., Matthews J. M., Cameron C. et al., 2006, Commun. Asteroseismol., 148, 34
Scargle J. D., 1982, ApJ 263, 835
Schmidt-Kaler T., 1982, w'Landolt-Börnstein', Vol 2b Group IV. Springer-Verlag, Berlin
Skrutskie M. F., Cutri R. M., Stiening R., Weinberg M. D., Schneider S. et al., 2006, AJ, 131, 1163
Suárez J.-C., Bruntt H., Buzasi D., 2005, A&A, 438, 633
Uytterhoeven K., Mathias P., Poretti E. et al., 2008, A&A 489, 1213
Uytterhoeven K., Briquet M., Bruntt H. et al. 2010a, AN, submitted
Uytterhoeven K., Szabo R., Southworth J. et al. 2010b, AN, submitted
van Leeuwen F., 2007, A&A, 474, 653
Voigt H. H., 2006, 'Landolt-Börnstein', Vol 3b Group VI. Springer-Verlag, Berlin
Warner P. B., Kaye A. B., Guzik J. A., 2003, ApJ, 593, 1049

This paper has been typeset from a TEX/LATEX file prepared by the author.